46th EPS Conference on Contr. Fusion and Plasma Phys., Milan, 8-12 July 2019

Unraveling the coupling of divertor closure and impurity radiation in the first impurity seeding experiments in the SAS divertor at DIII-D

L. Casali[1], T. H. Osborne[1], A. McLean[2], B. Covele[1], D. Eldon[1], B. Grierson[3], M. Shafer[4], D. Thomas[1], H. Wang[1], J. Watkins[5]

[1] *General Atomics, San Diego, USA*

[2] *Lawrence Livermore National Laboratory, USA*

[3] *Princeton Plasma Physics Laboratory, Princeton, USA*

[4] *Oak Ridge National Laboratory Oak Ridge, USA*

[5] *Sandia National Laboratory, Albuquerque, USA*

The first impurity seeding experiments in the Small Angle Slot (SAS) divertor in DIII-D have been carried out to study the interplay between divertor closure and impurity-induced dissipation. Future reactors will require high divertor radiation by impurity seeding [1, 2] and operation with some degrees of detachment to limit power loads on divertor components. It has been shown in a number of tokamaks [3, 4, 5, 6,7] that detachment onset can be influenced by variations in divertor target and baffle geometry. At DIII-D the role of divertor closure and target shaping for a highly dissipative divertor is currently being evaluated with the recently installed SAS slot [8,9]. The SAS includes a number of divertor design features combining a gas-tight slot geometry with a small target angle to bootstrap power and momentum dissipation of recycling neutrals [10] for achieving plasma detachment more compatible with core performance. The SAS slot is located near the main upper, outer divertor of DIII-D and is equipped with a comprehensive set of boundary diagnostics such as Langmuir probes (LPs), divertor Thomson scattering (DTS) system, ultraviolet wavelength spectrometer (DivSPRED), near infrared spectrometer (NIRS), and in-tile pressure gauges (PGs) (fig. 1 left). Experiments were performed in H-mode with I_p= 1.0 MA, B_t = 2 T with ion B×∇B directed into the SAS (toward the X-point in the upper divertor), and P_{NBI}=4.5 MW and 8MW with related density scans. In order to study the detachment dependence on strike point location, matched discharges with the same set of plasma parameters but with two different strike point locations were considered. In one case the strike point was located at the inner surface, and in the other case at the outer corner of the SAS (fig. 1 right). Impurities were injected at both the inner and outer corners of the SAS from two independent gas valves located at the same poloidal location but

at different toroidal locations (fig. 1 right) with the impurity flow split evenly between the two valves.

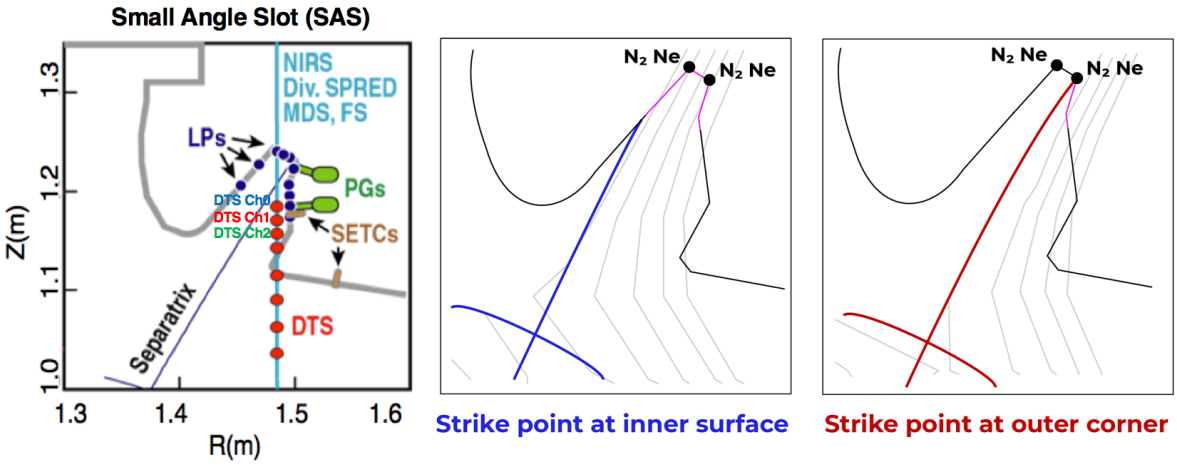

Figure 1. Left: The SAS slot in the upper divertor of DIII-D showing the comprehensive set of boundary diagnostics available. Right: The SAS divertor showing the two strike point locations used in the experiments (blue) and the position of the gas valves from which the impurities were injected (magenta).

Figure 2 shows time traces of input power (fig. 2a), radiated power (fig. 2 b), electron density (fig.2c), nitrogen puff (fig. 2d), and neutral pressure (fig. 2 e-f) for a discharge in which N_2 is injected at t=3.0 sec in the plasma from the corner valves and then its level is further raised at t=4.0 sec to invoke full detachment. As expected, the radiated power increases with N_2, while the discharge keeps a very stable behavior throughout. As soon as nitrogen is injected, a significant neutral pressure rise (p_0> 10 mtorr), which has been shown to correlate with the detachment onset [10], is detected by both the pressure gauges, hence in two different locations in the SAS. Langmuir probes measurements show the roll-over of the J_{sat} profile at the outer target and T_e of only few eV during the highest N_2 level. The eroding thermocouples detect a roll-over in the surface temperature suggesting a reduction of the heat flux. A clear reduction in T_e with N_2 seeding is also detected by the different DTS channels which show a clear drop starting at t= 4.0 sec with $T_e \sim 0.5$ eV (fig. 2 right). Spectra from the DivSPRED shows the bright resonance N_2 emission lines, the widening of the Lyman alpha and the appearance of the Lyman beta all features which indicate that T_e is below 2 eV. The NIRS spectrometer registers the appearance of the Paschen series of D lines which also coincides with $T_e < 2$ eV. The simultaneous observation of plasma cooling on the multiple diagnostics listed above suggest that the detachment front is not a highly local phenomenon but it rather extends through the entire slot. Interestingly, in matched nitrogen discharges with different strike point locations, the detachment onset requires different N_2 levels highlighting an important dependence of detachment on strike point location in the SAS as demonstrated, among other diagnostics, by

LPs measurements (fig. 3). When the strike point is located at the outer corner of the SAS (red), the J_{sat} (fig. 3 left) and T_e (fig. 3 right) drops occur only in correspondence of the highest N_2 puff rate (N_2 flow rate = 5 TorrL/s from each valve for a total flow rate of 10 TorrL/s), but when the strike point is located at the inboard side (blue), J_{sat} and T_e react promptly to even the lower N_2 rate (N_2 flow rate = 2.5 TorrL/s from each valve for a total flow rate of 5 TorrL/s).

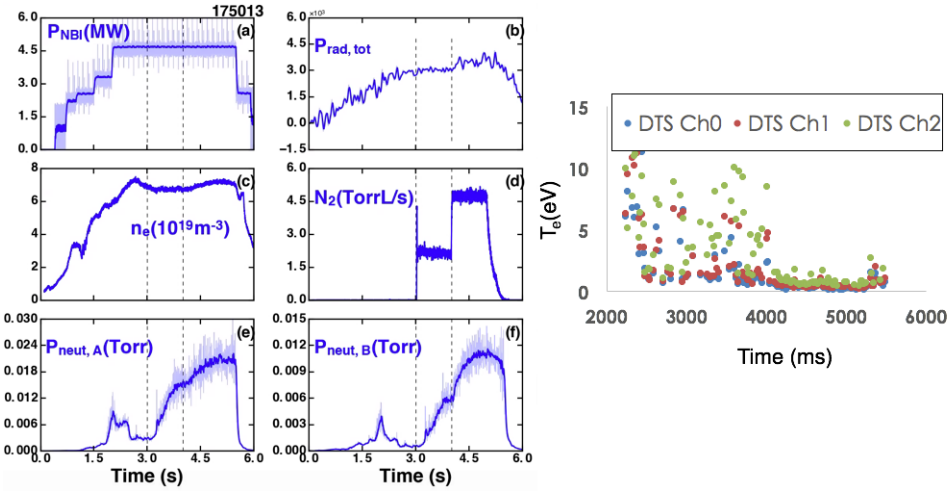

Figure 2. Left: Time traces of injected power (a), radiated power (b), electron density (c), nitrogen puff rate (d), neutral pressure (e-f). The dashed lines mark the time windows with the small N_2 puff (3.0-4.0s) and the high N_2 puff (4.0-6.0s). Right: Electron temperature from the DTS channels looking into the SAS as shown in fig1.

Such strike point dependence is also confirmed by the different nitrogen content reaching the core as indicated by both the core CER and SPRED measurements.

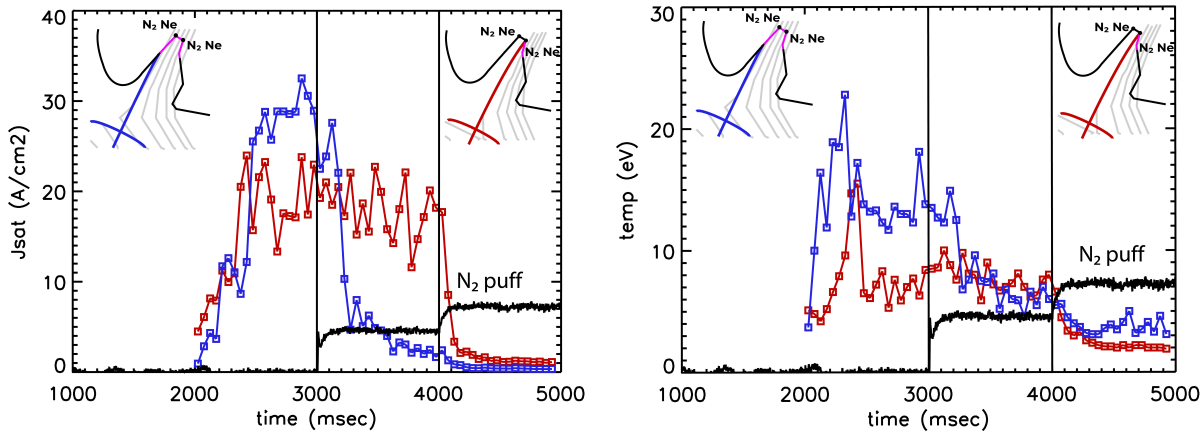

Figure 3. Left: Time traces of J_{sat} (left) and T_e (right) for two matched N2 discharges with different strike point locations.

The two strike point locations considered in these experiments correspond to different wetted target shapes and thus different distribution for the recycling source. When the strike point is located on the inboard side, the recycled ion flux is directed towards the outer SAS surface where it is reflected back to the strike point to enhance recycling. The results obtained with these two different strike points demonstrate that target shaping can affect dissipation by

redistributing the recycling source [10, 12] and hence affecting divertor detachment. In addition to N_2, the effect of Ne seeding in the SAS was also investigated. The neon discharge was designed such to match the input parameters, n_e and total P_{rad} from a selected N_2 discharge. Comparison of these two matched discharges reveals that while N_2 seeding does not significantly impact the core, Ne leads to higher pressure gradients than the unseeded cases as shown in fig. 4. A detailed pedestal and divertor analysis for the N_2 and Ne matched cases is ongoing. In conclusion, the first impurity seeding experiments in the new SAS divertor at DIII-D have shown the simultaneous observation of detachment on the entire boundary diagnostic suite viewing the SAS with stable discharge behavior and unchanged or improved pedestal performance. The dependence of detachment on strike point location suggests that the neutral and impurity distribution in the divertor can be controlled through variations in strike point location in a fixed baffle structure with important consequences for divertor dissipation.

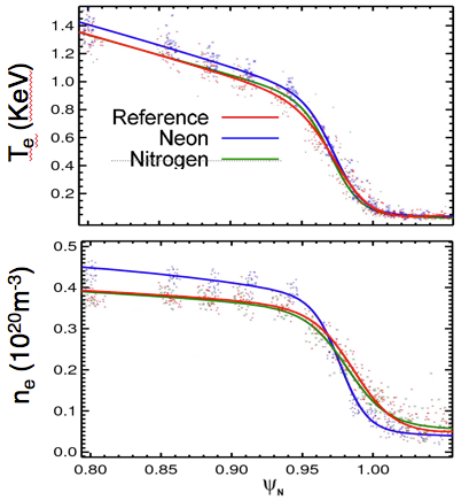

Figure 4: T_e and n_e profiles for unseeded case (red), N_2 case (green), Ne (blue)

References

[1] A. Kallenbach et al. Plasma Phys. Control. Fusion**, 55, 12** (2013)
[2] L. Casali et al. Phys. Plasmas **25,** 032506, (2018)
[3] B. Lipschultz et al. Fus.Sci.Technol. **51**, 363 (2007)
[4] S. Allen et al. Nucl. Fusion 39 2015 (1999)
[5] R. Neu et al. Nucl. Fusion **43**, 1191-6 (2003)
[6] A. Moser et al. submitted to Phys. Plasmas (2019)
[7] L. Casali et al. Contrib. to Plasma Phys 10 1002 (2018)
[8] C.F. Sang et al. Nucl. Fusion 75, 056043 (2017)
[9] H.Y. Guo et al. Nucl.Fusion https://doi.org/10.1088/1741-4326/ab26ee (2019)
[10] L. Casali et al. Nucl. Mater. Energy **19**, 537-543 (2019)
[11] M.W. Shafer et al. Nucl. Mater. Energy **19**, 487-492 (2019)
[12] B.M. Covele et al. to be submitted to Nucl.Fusion (2019)

Work supported by US DOES under DE-FC02-04ER54698 (DIII-D), DE-AC52-07NA27344 (LLNL), DE-AC02-09CH11466 (PPPL), and DE-AC05-00OR22725 (ORNL), DE-NA0003525 (SNL) and LDRD project 17-ERD-020. **Disclaimer:** This report was prepared as an account of work sponsored by an agency of the United States Government. Neither the United States Government nor any agency thereof, nor any of their employees, makes any warranty, express or implied, or assumes any legal liability or responsibility for the accuracy, completeness, or usefulness of any information, apparatus, product, or process disclosed, or represents that its use would not infringe privately owned rights. Reference herein to any specific commercial product, process, or service by trade name, trademark, manufacturer, or otherwise does not necessarily constitute or imply its endorsement, recommendation, or favoring by the United States Government or any agency thereof. The views and opinions of authors expressed herein do not necessarily state or reflect those of the United States Government or any agency thereof.